ORIGINAL PAPER

CrossMark

Trends in observed mean and extreme precipitation within the Yellow River Basin, China

Yang Zhao[1,2] · Xiangde Xu[2] · Wubin Huang[3] · Yuhong Wang[4] · Yanling Xu[5] · Hong Chen[6] · Zhaoping Kang[7]

Abstract

We analyzed spatiotemporal precipitation trends within the Yellow River Basin (YRB) in China and examined the connection between the changes in average and extreme precipitation indices. Data from 423 weather stations recorded from 1961 to 2016 were analyzed using the Mann-Kendall test to explore the linear trends of relationships between various indices, along with a simple linear regression used to detect monotonic positive or negative trends in the annual and seasonal precipitation data. Moreover, we divided the YRB into three distinct topographic regions to better understand the effect of regional geography on precipitation patterns. Our results demonstrated that mean precipitation and extreme precipitation days in different areas of the YRB had different variation trends. Precipitation in the YRB overall showed a negative trend, as did extreme precipitation days in the lower YRB. Mean and extreme precipitation indices were significantly correlated both annually and seasonally. These results may be helpful in preparing for both drought and flood events.

Keywords Yellow River · Trend analysis · Extreme precipitation · Correlation analysis · China

1 Introduction

Extreme weather events, such as frequent droughts and floods, have profound impacts on both economic and human welfare (Xia et al. 2015). Extreme precipitation events are among the most deadly and destructive natural disasters worldwide (Plummer et al. 1999; Potop et al. 2014) and the corresponding losses of life and property have demonstrated the importance of relevant research (Easterling et al. 2000). Although most such events have negative influences, extreme precipitation may be beneficial in some situations (Meehl et al. 2000). Many numerical experiments have shown that the number of extreme weather events may be more dependent on changes in climate variability than mean trends (Katz and Brown 1992). Thus, any subtle changes in the number or intensity of excessive events may have meaningful impacts on human society.

Changes in extreme rainfall patterns are vital indicators of climate change. Su et al. (2006) investigated extreme summer rainfall trends over the Yangtze River, China, and found that an increase in the number of rainstorm days, rather than intensity, was the main contributor to an observed upward precipitation trend in the Yangtze River Delta. Becker et al. (2006) concluded that monthly rainfall trends in the Yangtze River catchment were positively correlated with an increase in severe events in the area, leading to flood disasters in summer. Similarly, Wang et al. (2017) used gridded observation data with Coupled Model Intercomparison Project Phase 5 simulations based on the representative concentration pathway (RCP) 4.5 and 8.5 scenarios to analyze changes in average and excessive climate events in the arid region of northwestern China. Liu et al. (2008) indicated that annual

✉ Xiangde Xu
   xuxd@cma.gov.cn

1 Nanjing University of Information Science & Technology,
  Nanjing 210044, Jiangsu, China

2 State Key Laboratory of Severe Weather, Chinese Academy of
  Meteorological Sciences, Beijing 100081, China

3 Lanzhou Central Meteorological Observatory, Lanzhou 730020,
  China

4 Service Center of Public Meteorology, China Meteorological
  Administration, Beijing 100081, China

5 The Atmospheric Environment Department, Chinese Academy for
  Environmental Planning, Beijing 100012, China

6 Tianjin Meteorological Observatory, Tianjin 300074, China

7 Hubei Key Laboratory for Heavy Rain Monitoring and Warning
  Research, Institute of Heavy Rain, CMA, Wuhan 430074, China

precipitation in the Yellow River Basin (YRB) mainly showed a downward trend, and abrupt changes in the upstream and midstream regions occurred later than those in the downstream regions. Hu et al. (2012) noted a four-season pattern in the excessive rainfall trend, but only analyzed the YRB source region although the YRB flows from the Tibetan Plateau to eastern China and mountainous areas represent 67% of the basin's extent (Feng et al. 2007; Wang et al. 2010). In general, precipitation patterns are significantly affected by terrain (Shu et al. 2005; Liu et al. 2015; Henn et al. 2017; Stauffer et al. 2017) and the changing climate is sensitive to complex orographic effects in many parts of the world (Beniston 2003; Seidel and Free 2003). Thus, a detailed analysis of the trends in extreme climate events in China is important for reducing climate-induced flood and debris flow risks (Huang et al. 2013).

Previous studies mainly considered annual precipitation, ignoring the impact of seasonality (She et al. 2013; Jin et al. 2016). These studies indicated apparent trends in annual rainfall over the YRB (Liang et al. 2015; Cui et al. 2017), but failed to account for the connection between changes in average values and changes in extremes. Moreover, precipitation in the autumn and winter has a profound impact on the following spring's drought conditions. Thus, in this study, we analyzed both annual and seasonal precipitation for the entire YRB and three subregions and considered the connections between the changes in average and extreme rainfall values. Such detailed analysis and understanding of precipitation trend events in the YRB are important for predicting and mitigating floods and droughts.

2 Data and methods

2.1 Data

We employed the historic basic meteorology dataset, version 3.0, provided by the National Meteorological Information Center (NMIC) of the China Meteorological Administration (CMA); this consisted of 2474 gauge stations with daily precipitation records from 1961 to 2016. Although this dataset had previously undergone strict quality control measures including an extreme value check and internal consistency check by data providers, a further NMIC assessment found 35 gauge stations with inhomogeneity among the total 2474 stations (Shen and Xiong 2016). Most stations in the northwestern area of China were homogeneous (Yang and Li 2014).

The YRB contained 749 rainfall gauge stations, though we applied strict criteria to avoid missing values that could skew accurate results and removed stations with inconsistencies. For example, if a year's data contained < 3% missing days, it was considered sufficiently complete. Moreover, only

stations containing all 56 years of complete data from 1961 to 2016 were retained (Gao and Wang 2017). A total of 423 stations met these standards and were therefore selected to represent the spatiotemporal variations of precipitation over the YRB.

The number of days from January to December during which precipitation exceeded 50 mm (rainstorm) and 100 mm (downpour) and the number of days of non-storm precipitation (i.e., light rain that exceeded 0.1 mm, moderate rain that exceeded 10 mm, and heavy rain that exceeded 25 mm) were calculated for statistical purposes (Zhao et al. 2016). For seasonal analysis, we defined four seasons as spring (March–May, MAM), summer (June–August, JJA), autumn (September–November, SON), and winter (December–February, DJF) (Ali et al. 2015). In order to further analyze the spatial variability of precipitation, the area was divided into three parts (areas A, B, and C), based on the region's topographic "staircase" pattern of three distinct elevation regions (Fig. 1). There were 50 gauge stations in area A (the upper YRB, with altitudes greater than 2000 m), 181 gauge stations in area B (the middle YRB, with altitudes from 1000 to 2000 m), and 192 gauge stations in area C (the lower YRB, with altitudes less than 1000 m).

2.2 Methods

2.2.1 Precipitation index

We used annual (PreANU), seasonal (PreSEA), and monthly (PreMON) rainfall as mean precipitation indices (Table 1). The annual mean single-station precipitation was 16.8 mm over the entire YRB. The maximum annual single-station precipitation was 24.9 mm in 1964 and the minimum was
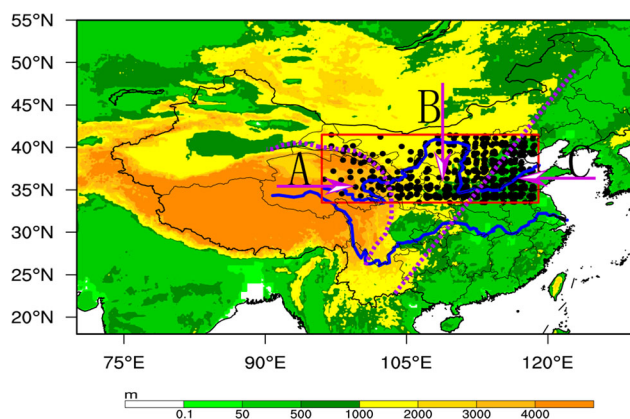
Fig. 1 Locations of 423 weather stations (black dots) along the Yellow River (blue line in the red box) used in the study area (red box, 33.5° N–41.5° N, 96° E–119° E). Terrain elevation is shown by color scale; purple dashed lines mark the rough boundaries of the three topographic regions forming the "staircase" pattern. Area A represents the upstream portion of the YRB, area B represents the midstream portion, and area C represents the downstream portion

Table 1 Definitions of mean and extreme rainfall indices

Index	Index name	Index definitions	Units
Mean	PreANU	Annual mean rainfall	mm
	PreSEA	Seasonal mean rainfall	mm
	PreMON	Monthly mean rainfall	mm
Extreme	PN01 (PNA01, PNB01, PNC01)	Number of days of rainfall ≥ 0.1 mm in the YRB (areas A–C)	days
	PN10 (PNA10, PNB10, PNC10)	Number of days of rainfall ≥ 10 mm in the YRB (areas A–C)	days
	PN25 (PNA25, PNB25, PNC25)	Number of days of rainfall ≥ 25 mm in the YRB (areas A–C)	days
	PN50 (PNA50, PNB50, PNC50)	Number of days of rainfall ≥ 50 mm in the YRB (areas A–C)	days
	PN100 (PNA100, PNB100, PNC100)	Number of days of rainfall ≥ 100 mm in the YRB (areas A–C)	days

12.4 mm in 1997. In areas A, B, and C, the annual mean single-station precipitation was 12.6 mm, 13.7 mm, and 20.8 mm, respectively. The maximum annual single-station precipitation was 17.1 mm, 19.5 mm, and 32.4 mm, respectively, while the minimum was 9.7 mm, 9.5 mm, and 14.8 mm. After considering the extreme climate indices proposed by previous research (e.g., Karl et al. 1999; Trenberth and Owen 1999; Zhang et al. 2005), we selected five indices for extreme precipitation analysis (Table 1): the number of days that daily precipitation was greater than 0.1 mm (PN01), 10 mm (PN10), 25 mm (PN25), 50 mm (PN50), and 100 mm (PN100), and we calculated these for the YRB overall and for each of the three subareas (Norrant and Douguédroit 2006; Pethybridge et al. 2009).

2.2.2 Trend test

The Mann-Kendall (M-K) test (Mann 1945; Kendall 1975; Gilbert 1987) is used to determine whether a variable follows a positive or negative trend over time. A monotonic positive (negative) trend shows that the variable consistently increases (decreases) over time, but the linear trend is not always clear. The M-K test is used for parametric linear regression analysis and examines whether a non-zero trend is present in the gradient of the estimated linear regression line. Most regression analysis assumes that fitted regression line residuals are normally distributed, but the M-K test is a distribution-free test that does not require such an assumption.

The M-K test is depended on the relative ranking of the data values. The M-K statistic S, used to estimate the significance, is calculated as (Wang and Swail 2001; Jung et al. 2015):

$$S = \sum_{i=1}^{n-1}\sum_{k=i+1}^{n} \mathrm{sgn}(x_k - x_i) \quad \mathrm{sgn}(x) = \begin{cases} 1\,(x_k - x_i) > 0 \\ 0\,(x_k = x_i) \\ -1\,(x_k - x_i) \end{cases}, \quad (1)$$

where x_k and x_i are continuous information values, and n is the size of the dataset. If S is above zero, observed values will increase over time while variable values will decrease over time. The variance of S is given by:

$$V_S^2 = \frac{n(n-1)(2n+5) - \sum_{i=1}^{m} e_i(e_{i-1})(2e_i+5)}{18}, \quad (2)$$

where m is the number of tied groups and e_i is the number of observations in the m group. The Z_{MK} (M-K test statistic) is calculated as:

$$Z_{MK} = \begin{cases} \dfrac{S-1}{V_S}, S > 0 \\ 0, S = 0 \\ \dfrac{S+1}{V_S}, S < 0 \end{cases}. \quad (3)$$

An above-zero (below-zero) value of Z_{MK} illustrates that the data have a positive (negative) trend over time. In the null hypothesis H_0, S is expected to have a normal distribution and should display no trend over time, while Z_{MK} is accepted if $|Z_{MK}| \geq |Z_{1-\alpha/2}|$, where $\mp Z_{1-\alpha/2}$ indicate the standard normal deviates and α is the significance level for the test (Im et al. 2011).

3 Results and analysis

3.1 Average rainfall trends

Figure 2 shows the PreANU variations in the entire YRB region and areas A, B, and C from 1961 to 2016. The overall mean annual precipitation had a downward trend with a 95% confidence level, as did areas B and C; only area A had an upward trend.

As for seasonal trends (Fig. 3, Table 2), all four seasons showed downward trends in the YRB overall, with summer

Fig. 2 Variations from 1961 to 2016 of inter-annual station mean precipitation (different colored lines and points) and trends (solid lines) in **a** the entire YRB, **b** area A, **c** area B, and **d** area C
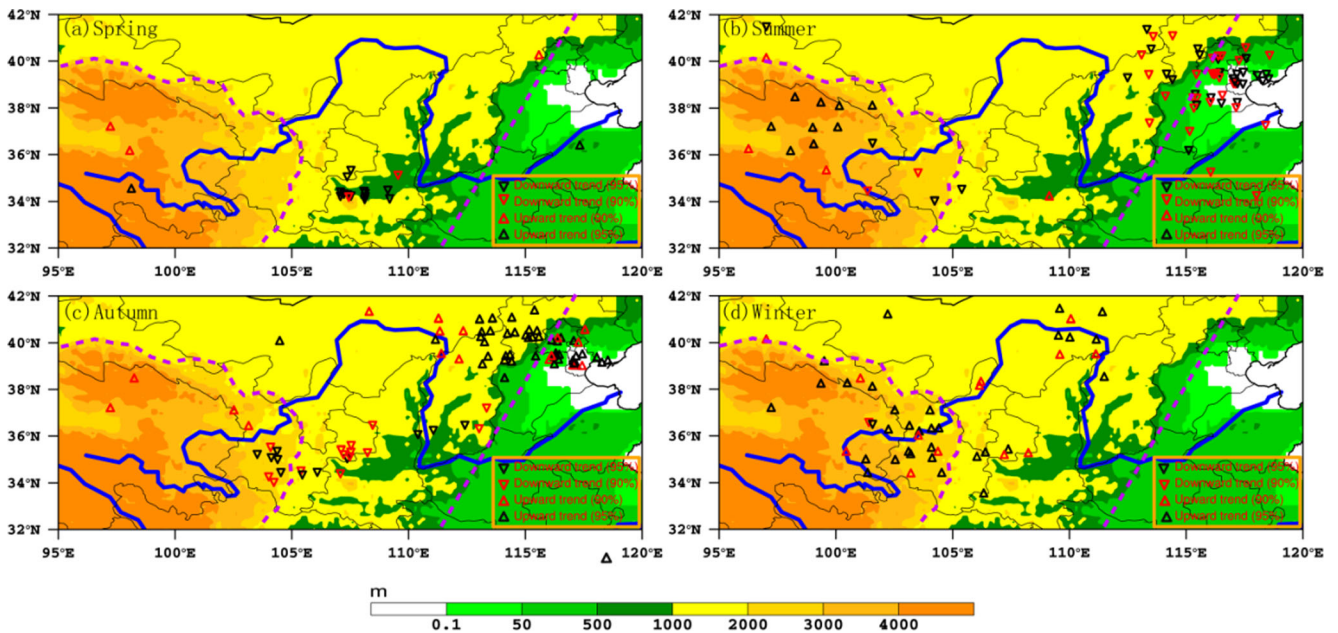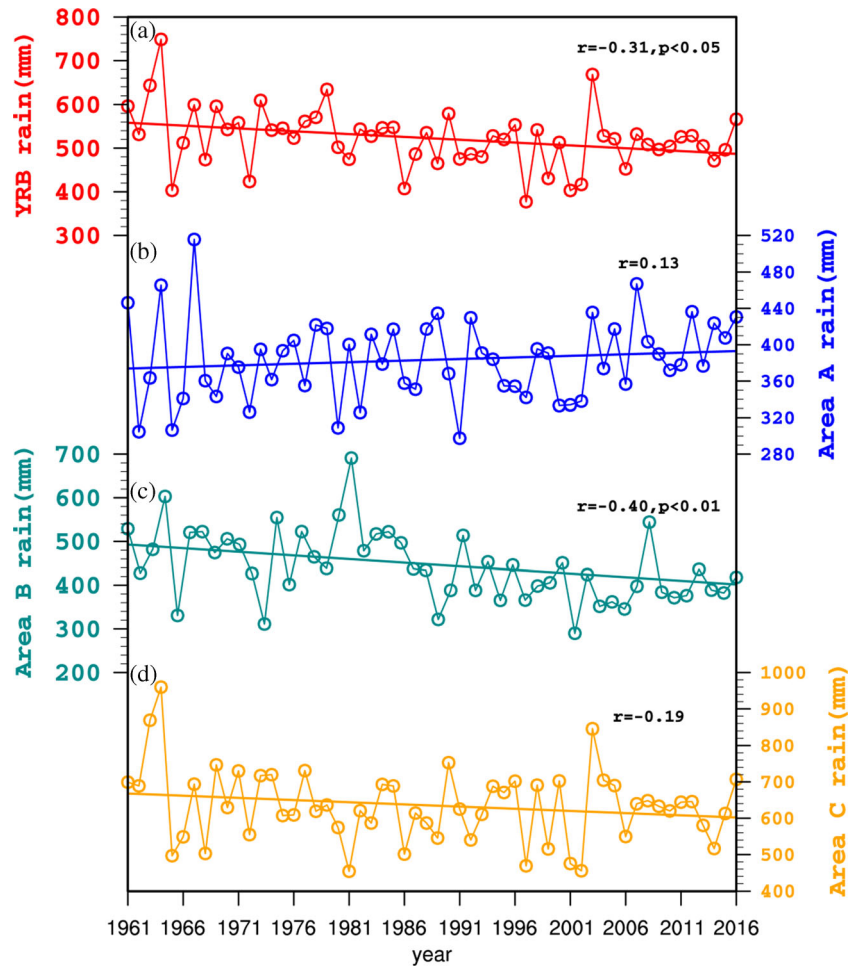
Fig. 3 Trends in seasonal precipitation from 1961 to 2016 determined using the Mann-Kendall test with 423 observation stations. Triangles indicate an upward or downward trend with at least 90% confidence. Blue line marks the course of the Yellow River. Terrain elevation is shown by color scale; purple dashed lines mark the rough boundaries of the three topographic regions forming the "staircase" pattern

Table 2 The Mann-Kendall test statistics for seasonal mean rainfall within the YRB and areas A–C for 1961–2016

	Year	Spring	Summer	Autumn	Winter
YRB	− 0.31**	− 0.06	− 0.22*	− 0.09	− 0.37**
Area A	0.13	0.07	0.07	− 0.03	0.29**
Area B	− 0.40**	− 0.15	− 0.12	− 0.19	− 0.37**
Area C	− 0.19	− 0.01	− 0.22*	0.01	− 0.15

*90% confidence level

**95% confidence level

and winter having 90 and 95% confidence levels, respectively. Area B was similar, though the summer trend was less pronounced. Area C showed negative trends in spring, summer, and winter, with the a summer trend at a 90% confidence level. In contrast, area A showed positive trends in spring, summer, and winter, the latter with a 95% confidence level.

Fifteen stations had negative springtime trends in area B at a 90% confidence level (Fig. 3a). Area C had negative summertime trends, with 44 stations trending at 90% confidence; area B also had 14 stations with the same negative trend at the same confidence level (Fig. 3b). Positive trends dominated areas B and C in the autumn, with 29 stations in the regions meeting the 90% confidence interval. These positive trends tended to be distributed near the transitional areas between different "staircase" zones (Fig. 3c). Areas A and B had 20 and 24 positively trending stations in the winter at the 90% confidence level, respectively (Fig. 3d).

3.2 Extreme rainfall trends

Analysis of the number of annual extreme rainfall (> 50 mm) days at stations located in the research area from 1961 to 2002 indicated negative trends. Every area had a downward trend from 1961 to 2002, all but area A at 90% confidence (Fig. 4). Additionally, the number of annual extreme precipitation days over the entire YRB, area A, and area C had slightly downward trends in recent years (2003–2016), while B showed inconsistent fluctuations.

Next, the five selected indices were employed for extreme precipitation analysis. PN01 in all three areas showed a downward trend from west to east (Fig. 5) but all other indices showed the opposite trend. Annually, area A did not achieve a precipitation mean of 50 mm, while area C was the only area to reach 100 mm. Seasonally, PN100 only occurred in area C in the spring (0.01 times) and summer (0.29 times). PN50 only occurred in areas B and C, especially in the summer and in the autumn; in the latter, PN50 occurred 1.7 times at the average gauge station in the summer and 0.21 times in the autumn.

Next, seasonal trends in extreme precipitation were evaluated. We found that 51 (58%) gauge stations had positive

trends in area B, and 96 (53%) gauge stations had positive trends in area C in the spring. There were a comparable number of positively (15, 83) and negatively (18, 88) trending gauge stations in area A and area B from summer to autumn. Area C had primarily negative summertime trends at 140 (73%) gauge stations; this trend continued into the autumn with 134 (70%) stations. Figure 6 shows that, in the analysis of extreme precipitation, 27 gauge stations had negative trends in area C during the summer, with at least 90% confidence. Area B and area C had 18 and 15 stations, respectively, with negative trends in the autumn, with at least a 90% confidence level.

3.3 The connection between mean and extreme rainfall indices

After analyzing the spatial and temporal characteristics of average and extreme rainfall levels in the YRB, we attempted to correlate the two. Most correlations met at least the 95% confidence limit (Table 3). In the spring and autumn, the degree of correlation was nearly equal for different areas and precipitation levels. Correlations of PN[ABC]01 were more significant in the spring and autumn than annually or in other seasons. In the summer and annually, the correlation of PNC25 was more significant, while in spring, autumn, and winter, PN[ABC]10 was relatively significant. The highest correlation between mean and extreme precipitation clearly occurred in summer over the YRB. The highest correlations were mainly concentrated in areas B and C.

4 Discussion and conclusions

The YRB was divided into three parts according to its three constituent "staircase" topographic features in order to facilitate regional climate change research. From both inter-annual and seasonal points of view, the spatiotemporal changes in mean and extreme precipitation over the YRB and its three sub-regions were analyzed from 1961 to 2016 using the M-K trend test on the basis of 423 rainfall gauge stations. The results showed that mean and extreme precipitation had different trends and distinct seasonal shifts over the whole basin and its sub-regions, leading to the following conclusions:

(1) The annual mean precipitation had a negative trend over the whole basin except the upper YRB. The seasonality trend of mean precipitation was evident over the YRB and it three sub-regions.

(2) Five indices were employed for precipitation extremes. Annual extreme precipitation days over the whole basin and three sub-regions had a consistent downward trend from 1961 to 2002. From 2003 to 2016, rainstorm days over the whole basin and sub-regions had a slightly
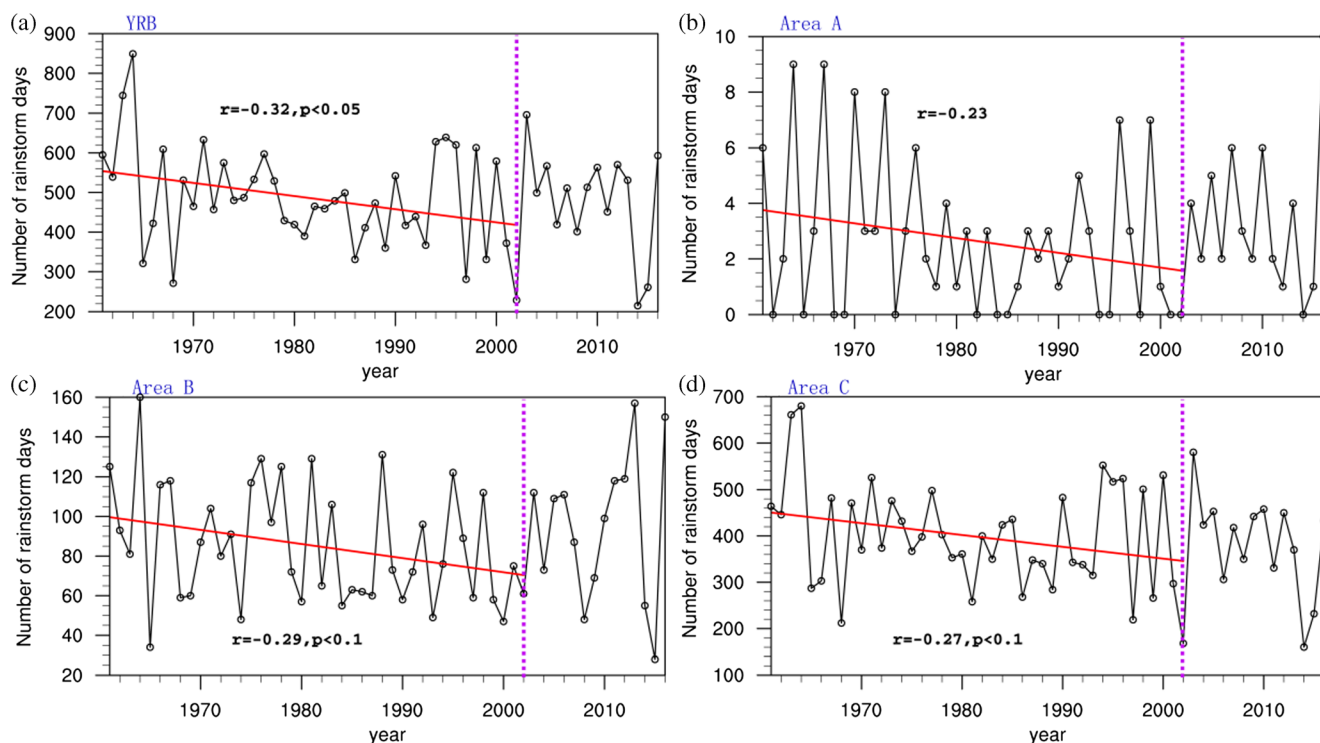
Fig. 4 Inter-annual variations (black lines and points) and trends (solid red lines) in the number of extreme precipitation days (> 50 mm) at stations located in **a** the YRB, **b** area A, **c** area B, and **d** area C from 1961 to 2016. The vertical axes represent the total rainstorm days at all stations in the different areas

downward trend except in the middle YRB. Spatially, rainstorms days increased from west to east over the YRB in every, and rainstorms days were mainly concentrated in the middle-lower reaches of the YRB, especially in the summer and autumn. The trends of extreme precipitation days also showed obvious seasonality over the whole basin and three sub-regions.

(3) Relationships between mean precipitation and rainstorm days were investigated in different regions and seasons. Every extreme precipitation index had a significant positive correlation with mean precipitation in the corresponding region and season; the highest positive correlation occurred over the middle-lower YRB in the summer.

Other research has detected variations in mean precipitation and extremes over the YRB (e.g., Yang and Chunhui 2004; Li et al. 2011; Ma et al. 2013). Xu and Zhang (2006) identified a downward trend of annual mean precipitation over the YRB in the past 50 years from 77 stations. Liu et al. (2008) found that an upward trend of annual mean precipitation was significant in the upper reaches of the YRB, while downstream areas showed the opposite trend based on 81 stations. Zhang et al. (2014) confirmed these annual mean precipitation patterns over the whole YRB and sub-regions from 64 rainfall stations and found a downward trend over the whole YRB in

the spring and autumn. Although our results matched such previous research, we investigated and discussed the seasonality of mean precipitation in every sub-region of the YRB in more detail on the basis of 423 observation stations, a higher level of detail than previously reported.

Furthermore, Dong et al. (2011) used a generalized linear model to report a significant downward trend in annual extreme precipitation over the central-east YRB with 215 stations from 1951 to 2004. Gao and Wang (2017) reported an enhanced rainfall extreme intensity but a declining extreme precipitation days in the middle-lower YRB. Hu et al. (2012) proposed a varying seasonality of extreme precipitation across the YRB based on only 17 widely distributed stations and highlighted a negative extreme precipitation trend in the summer. At an inter-annual scale, our results clearly showed annual extreme precipitation trends over the whole basin and three sub-regions, but also detected spatial patterns from west to east over the YRB. At a seasonal scale, we reported varying seasonal trends of extreme precipitation with a negative trend over the middle-lower YRB in the summer and autumn, new information not reported by the previous research.

Finally, though previous research compared mean precipitation and extreme precipitation days over the YRB and sub-regions using only 62 meteorological stations (Liang et al. 2015), the relationship between the two remained unclear. Our results highlighted their significant
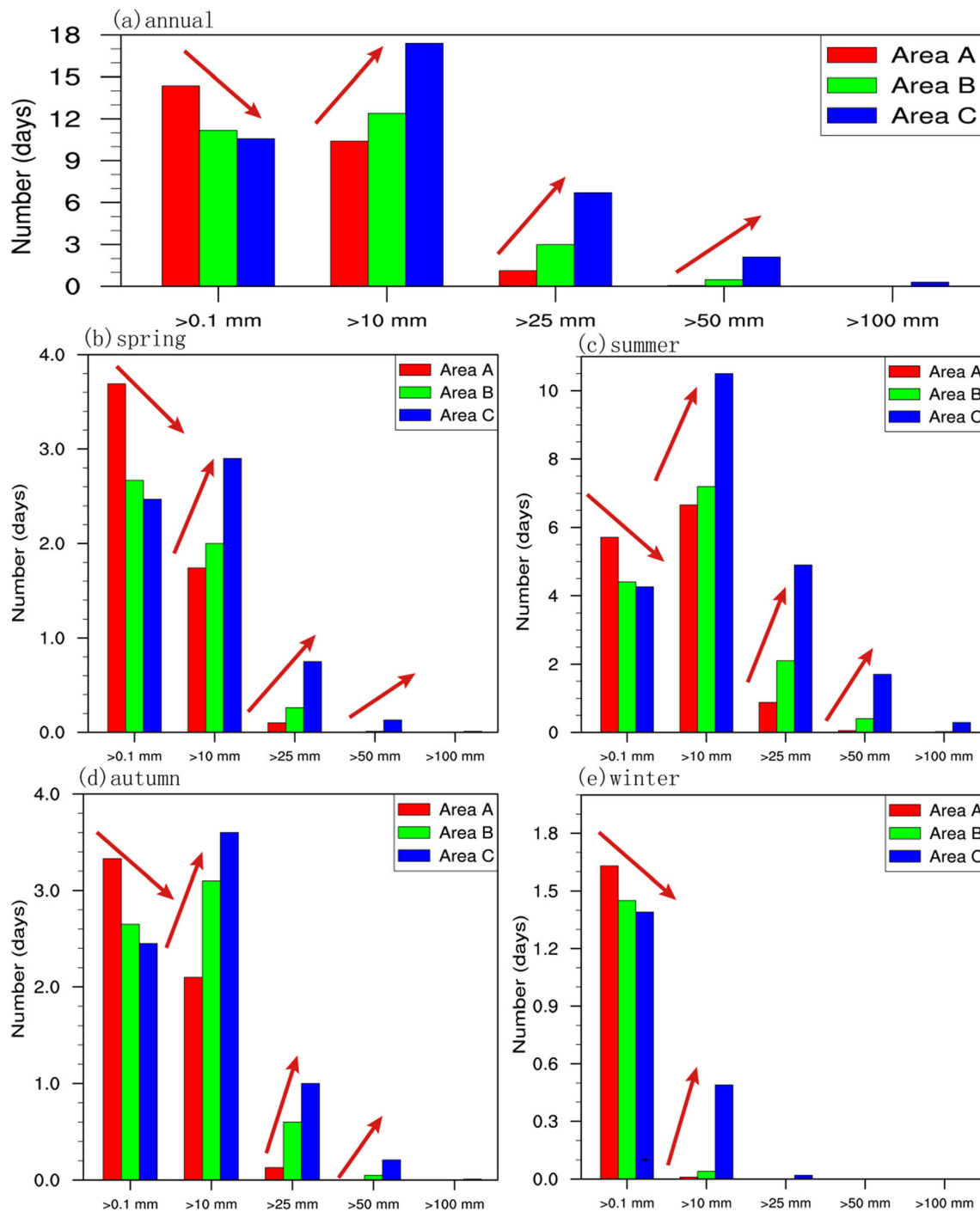
Fig. 5 Number of precipitation days of different levels (PN01, PN10, PN25, PN50, and PN100) at gauge stations within the three areas annually and seasonally from 1961 to 2016. Red arrow indicates the trend in rainfall values across the three areas. Values for 0.1 mm have been reduced by a factor of 10 to improve the figure's legibility

positive relationship over the YRB and sub-regions at seasonal and inter-annual scales.

Our results could play a crucial role in water resource management, agriculture, human activities, and further studies of regional climate change in arid and semi-arid regions of China. The annual mean precipitation results indicate a drought tendency in the central-east YRB, while the western parts of the YRB may experience alleviated water resource shortages. Further research on mean precipitation in different regions and seasons would assist the sustainable development of the YRB and provide efficient fresh water utilization in the north of China. In addition,
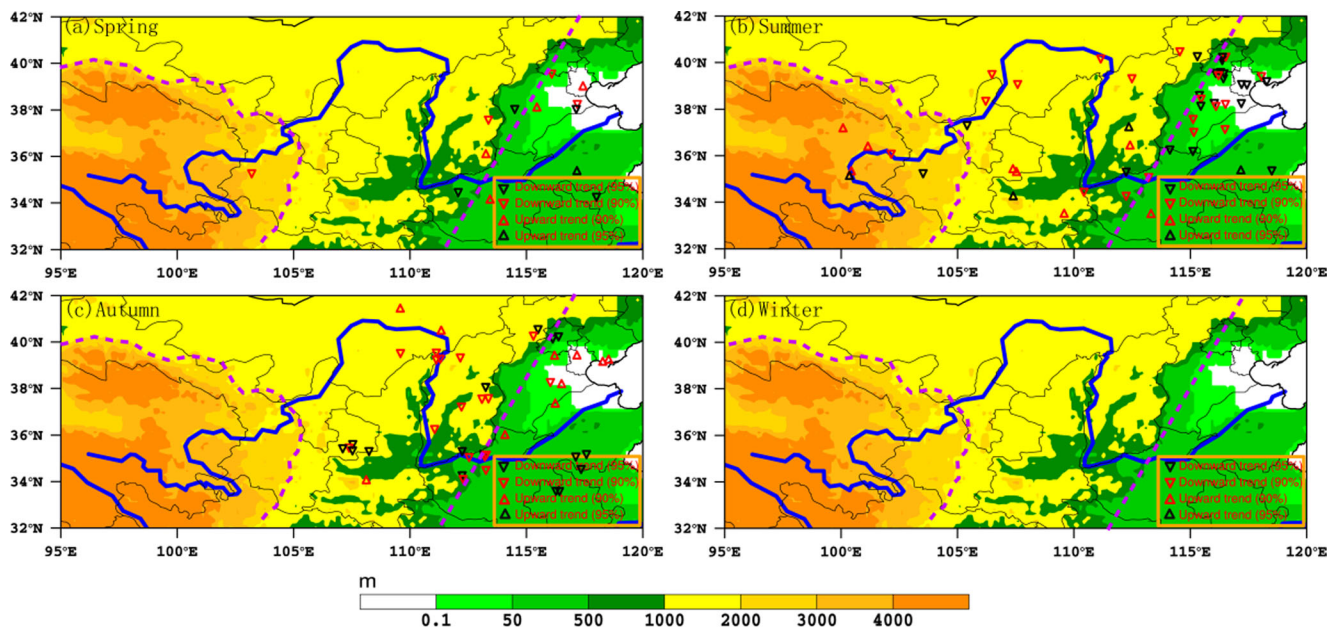
Fig. 6 Trends in the number of seasonal extreme precipitation (> 50 mm) days determined using the M-K test from 1961 to 2016. Triangles indicate an upward or downward trend with at least 90% confidence. Blue line marks the course of the Yellow River. Terrain elevation is shown by color scale; purple dashed lines mark the rough boundaries of the three topographic regions forming the "staircase" pattern

the association of extreme and mean precipitation implies that, once summer rainfall begins to occur over the middle-lower YRB, it may tend to develop into heavier rainstorms

Table 3 Correlation coefficients between average precipitation and extreme rainfall days

Indicator		Spring	Summer	Autumn	Winter	Annual
YRB	PN01	0.74**	0.60**	0.74**	0.28*	0.55**
	PN10	0.97**	0.96**	0.98**	0.37**	0.92**
	PN25	0.93**	0.98**	0.92**	0.17	0.90**
	PN50	0.66**	0.92**	0.68**	None	0.78**
	PN100	0.14	0.61**	0.37**	None	0.45**
Area A	PNA01	0.51**	0.39**	0.79**	− 0.001	0.29*
	PNA10	0.95**	0.97**	0.95**	− 0.005	0.93**
	PNA25	0.58**	0.76**	0.59**	None	0.69**
	PNA50	None	0.44**	None	None	0.50**
	PNA100	None	None	None	None	None
Area B	PNB01	0.73**	0.60**	0.68**	0.07	0.56**
	PNB10	0.93**	0.98**	0.91**	0.04	0.74**
	PNB25	0.88**	0.94**	0.76**	None	0.68**
	PNB50	0.53**	0.78**	0.39**	None	0.47**
	PNB100	None	0.40**	None	None	0.16
Area C	PNC01	0.76**	0.68**	0.75**	0.68**	0.55**
	PNC10	0.97**	0.95**	0.97**	0.74**	0.94**
	PNC25	0.95**	0.98**	0.95**	0.36**	0.96**
	PNC50	0.69**	0.96**	0.77**	None	0.90**
	PNC100	0.31*	0.71**	0.43**	None	0.63**

*90% confidence level; **95% confidence level. "None" means no value

despite the overall downward rainfall trend in these regions. This phenomenon would complicate attempts at forecasting extreme weather.

Additionally, some past research has attributed precipitation across the YRB to large-scale external forcing. Gao and Wang (2017) claimed that extreme precipitation variations over the YRB were associated with elevation and the East Asian summer monsoon. Li et al. (2016) showed that precipitation patterns in the YRB were mainly affected by topographic factors and atmospheric water sources. Liang et al. (2015) explored the relationship between monthly extreme precipitation indices and subtropical highs in the Northern Hemisphere. However, as the possible causes of the seasonal and annual characteristics of mean and extreme precipitation across the YRB reported here are unclear, further research into this question is warranted.

References

Ali S, Dan L, Fu C, Yang Y (2015) Performance of convective parameterization schemes in Asia using RegCM: simulations in three typical regions for the period 1998–2002. Adv Atmos Sci 32(5):715–730. https://doi.org/10.1007/s00376-014-4158-4

Becker S, Gemmer M, Jiang T (2006) Spatio-temporal analysis of precipitation trends in the Yangtze River catchment. Stoch Env Res Risk A 20(6):435–444. https://doi.org/10.1007/s00477-006-0036-7

Beniston M (2003) Climatic change in mountain regions: a review of possible impacts. Clim Chang 59(1–2):5–31. https://doi.org/10.1023/A:1024458411589

Cui L, Wang L, Lai Z, Tian Q, Liu W, Li J (2017) Innovative trend analysis of annual and seasonal air temperature and rainfall in the Yangtze River Basin, China during 1960–2015. J Atmos Sol Terr Phys 164:48–59. https://doi.org/10.1016/j.jastp.2017.08.001

Dong Q, Chen X, Chen T (2011) Characteristics and changes of extreme precipitation in the Yellow-Huaihe and Yangtze-Huaihe Rivers Basins, China. J Clim 24(14):3781–3795. https://doi.org/10.1175/2010JCLI3653.1

Easterling DR, Meehl GA, Parmesan C, Changnon SA, Karl TR, Mearns LO (2000) Climate extremes: observations, modeling, and impacts. Science 289(5487):2068–2074. https://doi.org/10.1126/science.289.5487.2068

Feng Z, Tang Y, Yang Y, Zhang D (2007) The relief degree of land surface in China and its correlation with population distribution. Acta Geogr Sin 62(10):1073–1082. https://doi.org/10.11821/xb200710007 (in Chinese)

Gao T, Wang H (2017) Trends in precipitation extremes over the Yellow River basin in North China: changing properties and causes. Hydrol Process 31(13):2412–2428. https://doi.org/10.1002/hyp.11192

Gilbert RO (1987) Statistical methods for environmental pollution monitoring. Wiley, New York

Henn B, Newman AJ, Livneh B, Daly C, Lundquist JD (2017) An assessment of differences in gridded precipitation datasets in complex terrain. J Hydrol 556:1205–1219. https://doi.org/10.1016/j.jhydrol.2017.03.008

Hu Y, Maskey S, Uhlenbrook S (2012) Trends in temperature and rainfall extremes in the Yellow River source region, China. Clim Chang 110(1–2):403–429. https://doi.org/10.1007/s10584-011-0056-2

Huang J, Sun S, Zhang J (2013) Detection of trends in precipitation during 1960–2008 in Jiangxi province, southeast China. Theor Appl Climatol 114(1–2):237–251. https://doi.org/10.1007/s00704-013-0831-2

Im ES, Jung IW, Bae DH (2011) The temporal and spatial structures of recent and future trends in extreme indices over Korea from a regional climate projection. Int J Climatol 31(1):72–86. https://doi.org/10.1002/joc.2063

Jin L, Wang C, Wang P et al (2016) Analysis of characteristics of the extreme precipitation in the Yellow river basin. J Water Resour Water Eng 27(6):50–60 (in Chinese)

Jung IW, Bae DH, Kim G (2015) Recent trends of mean and extreme precipitation in Korea. Int J Climatol 31(3):359–370. https://doi.org/10.1002/joc.2068

Karl TR, Nicholls N, Ghazi A (1999) Clivar/GCOS/WMO workshop on indices and indicators for climate extremes workshop summary. Clim Chang 42(1):3–7. https://doi.org/10.1023/A:1005491526870

Katz RW, Brown BG (1992) Extreme events in a changing climate: variability is more important than averages. Clim Chang 21(3):289–302. https://doi.org/10.1007/BF00139728

Kendall MG (1975) Rank correlation methods, 4th edn. Charles Griffin, London

Li MJ, Hou XY, Ying LL (2011) Spatial-temporal dynamics of NDVI and its response to temperature and precipitation in the Yellow River Delta during the period 1998–2008. Resour Sci 33(2):322–327 (in Chinese)

Li Q, Yang M, Wan G, Wang X (2016) Spatial and temporal precipitation variability in the source region of the Yellow River. Environ Earth Sci 75(7):594. https://doi.org/10.1007/s12665-016-5583-8

Liang K, Liu S, Bai P, Nie R (2015) The Yellow River basin becomes wetter or drier? The case as indicated by mean precipitation and extremes during 1961–2012. Theor Appl Climatol 119(3–4):701–722

Liu Q, Yang Z, Cui B (2008) Spatial and temporal variability of annual precipitation during 1961–2006 in Yellow River Basin, China. J Hydrol 361(3–4):330–338. https://doi.org/10.1016/j.jhydrol.2008.08.002

Liu M, Xu X, Sun AY, Wang K, Yue Y, Tong X, Liu W (2015) Evaluation of high-resolution satellite rainfall products using rain gauge data over complex terrain in southwest China. Theor Appl Climatol 119(1–2):203–219. https://doi.org/10.1007/s00704-014-1092-4

Ma XN, Zhang M, Qian MA, Liu W (2013) Nonuniform change of precipitation in Yellow River Basin during flood period. J Nat Disasters 22(4):92–100

Mann HB (1945) Non-parametric tests against trend. Econometrica 13:163–171

Meehl GA, Karl T, Easterling DR, Changnon S, Pielke R Jr, Changnon D, Evans J, Groisman PY, Knutson TR, Kunkel KE, Mearns LO, Parmesan C, Pulwarty R, Root T, Sylves RT, Whetton P, Zwiers F (2000) An introduction to trends in extreme weather and climate events: observations, socioeconomic impacts, terrestrial ecological impacts, and model projections. Bull Am Meteorol Soc 108(3):46–51. https://doi.org/10.1175/1520-0477(2000)081<0413:AITTIE>2.3.CO;2

Norrant C, Douguédroit A (2006) Monthly and daily precipitation trends in the Mediterranean (1950–2000). Theor Appl Climatol 83(1–4):89–106. https://doi.org/10.1007/s00704-005-0163-y

Pethybridge SJ, Gent DH, Esker PD, Turechek WW, Hay FS, Nutter FWJ (2009) Site-specific risk factors for ray blight in Tasmanian pyrethrum fields. Plant Dis 93(3):229–237. https://doi.org/10.1094/PDIS-93-3-0229

Plummer N, Salinger MJ, Nicholls N, Suppiah R, Hennessy KJ, Leighton RM, Trewin B, Page CM, Lough JM (1999) Changes in climate extremes over the Australian region and New Zealand during the twentieth century. Clim Chang 42(1):183–202. https://doi.org/10.1023/A:1005472418209

Potop V, Zahraniček P, Türkott L, Štěpánek P, Soukup J (2014) Risk occurrences of damaging frosts during the growing season of vegetables in the Elbe River lowland, the Czech Republic. Nat Hazards 71(1):1–19. https://doi.org/10.1007/s11069-013-0894-5

Seidel DJ, Free M (2003) Comparison of lower-tropospheric temperature climatologies and trends at low and high elevation radiosonde sites. Clim Chang 59(1–2):53–74. https://doi.org/10.1007/978-94-015-1252-7_4

She D, Xia J, Song J, Du H, Chen J, Wan L (2013) Spatio-temporal variation and statistical characteristic of extreme dry spell in Yellow River Basin, China. Theor Appl Climatol 112(1–2):201–213. https://doi.org/10.1007/s00704-012-0731-x

Shen Y, Xiong A (2016) Validation and comparison of a new gauge-based precipitation analysis over mainland China. Int J Climatol 36(1):252–265

Shu SJ, Yu ZF, Wang Y, Bai M (2005) A statistic model for the spatial distribution of precipitation estimation over the Tibetan complex terrain. Chin J Geophys 48(3):593–601. https://doi.org/10.1002/cjg2.692 (in Chinese)

Stauffer R, Mayr GJ, Messner JW, Umlauf N, Zeileis A (2017) Spatio-temporal precipitation climatology over complex terrain using a censored additive regression model. Int J Climatol 37(7):3264–3275. https://doi.org/10.1002/joc.4913

Su BD, Jiang T, Jin WB (2006) Recent trends in observed temperature and precipitation extremes in the Yangtze River basin, China. Theor Appl Climatol 83(1–4):139–151. https://doi.org/10.1007/s00704-005-0139-y

Trenberth KE, Owen TW (1999) Workshop on indices and indicators for climate extremes, Asheville, NC, USA, 3–6 June 1997 breakout group A: storms. Clim Chang 42(1):9–21. https://doi.org/10.1023/A:1005443610940

Wang XL, Swail VR (2001) Changes of extreme wave heights in northern hemisphere oceans and related atmospheric circulation regimes. J Clim 14(10):2204–2221. https://doi.org/10.1175/1520-0442(2001)014<2204:COEWHI>2.0.CO;2

Wang Z, Hu Z, Liu H, Gong H, Zhao W, Yu M, Zhang M (2010) Application of the relief degree of land surface in landslide disasters susceptibility assessment in China. 18th International Conference on Geoinformatics. IEEE, pp 1–5. https://doi.org/10.1109/GEOINFORMATICS.2010.5567734

Wang Y, Zhou B, Qin D, Wu J, Gao R, Song L (2017) Changes in mean and extreme temperature and precipitation over the arid region of northwestern China: observation and projection. Adv Atmos Sci 34(3):289–305. https://doi.org/10.1007/s00376-016-6160-5

Xia F, Liu X, Xu J, Wang Z, Huang J, Brookes PC (2015) Trends in the daily and extreme temperatures in the Qiantang River basin, China. Int J Climatol 35(1):57–68. https://doi.org/10.1002/joc.3962

Xu ZX, Zhang N (2006) Long-term trend of precipitation in the Yellow River basin during the past 50 years. Geogr Res 25(1):27–34 (in Chinese)

Yang Z, Chunhui LI (2004) The spatial and temporal structure of precipitation in the Yellow River Basin. Prog Geogr 23(2):27–33. https://doi.org/10.11820/dlkxjz.2004.02.004

Yang S, Li QX (2014) Improvement in inhomogeneity analysis method and update of China precipitation data. Adv Clim Chang Res 10(4):276–281 (in Chinese)

Zhang X, Aguilar E, Sensoy S, Melkonyan H, Tagiyeva U, Ahmed N (2005) Trends in Middle East climate extreme indices from 1950 to 2003. J Geophys Res Atmos 110(D22):3159–3172. https://doi.org/10.1029/2005JD006181

Zhang Q, Peng J, Singh VP, Li J, Chen YD (2014) Spatio-temporal variations of precipitation in arid and semiarid regions of China: the Yellow River basin as a case study. Glob Planet Chang 114(2):38–49

Zhao Y, Xu XD, Zhao TL, Xu HX, Mao F, Sun H, Wang YH (2016) Extreme precipitation events in East China and associated moisture transport pathways. Sci China Earth Sci 59(9):1–19. https://doi.org/10.1007/s11430-016-5315-7